Int. J. Electrochem. Sci., 12 **(2017)** 11287 – 11297, doi: 10.20964/2017.12.63

International Journal of
ELECTROCHEMICAL
SCIENCE
www.electrochemsci.org

Graphene Quantum Dots Doped PEDOT and Its Electrocatalytic Performance for Oxygen Reduction Reaction

Xiangyu Gao[1], *Jinfu Ma*[1,*], *Yingtao Li*[2,*] , *Haicheng Wei*[3]

[1] School of Material Science and Engineering, North Minzu University, Yinchuan 750021, China
[2] School of Physical Science and Technology, Lanzhou University, Lanzhou 730000, China
[3] School of Electrical and Information Engineering, North Minzu University, Yinchuan 750021, China
[*]E-mail: li_yt06@lzu.edu.cn, jinfu_ma@163.com

Received: 7 September 2017 / *Accepted:* 21 October 2017 / *Published:* 12 November 2017

Oxygen reduction reaction (ORR) is key issue for fuel cells because it always produces large polarization thus result in decrease of fuel cell performance. Herein, poly(3,4-ethylenedioxythiophene) (PEDOT) doped with graphene quantum dots (GQDs) was explored as an efficient ORR catalyst. GQDs with size of 3-5 nm were prepared by thermal reduction at 200°C. The PEDOT and GQDs@PEDOT were prepared by electropolymerization. Morphology and structure of catalysts were characterized by TEM and Raman. The catalytic activity and stability were investigated by CV, LSV, RDE and CA. Physical characterization indicated that PEDOT had a catenulate structure and GQDs were successfully combined with PEDOT. The results of electrochemical tests showed that the reduction peak current density of ORR was clearly increased after GQDs doping. Calculated by the K-L equation, the number of transferred electrons at -0.6 V increased from 2.66 to 3.57, which closed to the theoretical value 4. CA tests indicated that the current density on GQDs@PEDOT electrode was 0.26 mA·cm^{-2}. The hybrid of GQDs with PEDOT can enhance the catalytic activity and stability for ORR.

Keywords: Oxygen reduction reaction; Poly(3,4-ethylenedioxythiophene); Graphene quantum dots; Electrocatalytic activity

1. INTRODUCTION

Fuel cell (FC), a new type of energy conversion device with high power density, low operating temperature and environmental-friendly emissions, has attracted extensive attentions as a potential power source in recent years[1, 2]. For FCs, the cathode catalyst involving the ORR is the key factor determining the fuel cell's performance. Due to the complex reaction mechanism and high driving

overpotential, ORR usually needs high active catalysts[3]. Till now, Pt and/or its alloy are well known as active and efficient catalysts for ORR, but the high price and limited resource obstruct their commercialization[4, 5]. Recently, a great number of promising candidates of non Pt-based catalysts have emerged such as transition metal oxides[6-8], N-containing transition metal catalysts absorbed on carbon support (Me-N-C, Me=Co, Fe, *etc*.)[9, 10]. Especially, metal-free ORR electrocatalysts have been widely explored for an alternative to Pt-based catalysts because of their low cost, high activity, enhanced stability and improved fuel tolerance[1, 11-16]. Gong and co-workers[17] reported that N-doped C nanotubes and graphene had high electrocatalytic activity for ORR with enhanced durability. Winther-Jensen *et al*.[18] reported an air electrode based on a porous material coated with PEDOT, which acts as an ORR catalyst without material degradation or deterioration. It could work for 1500 h. However, some major challenges still obstruct the practical applications of these metal-free catalysts, such as the rigorous reaction conditions, tedious procedures, and special instruments[19]. Thus, the development of a new type of metal-free ORR catalysts under mild conditions can be considered to be one of the highest priorities in the development of FCs[19]. Our previous paper[20] prepared the PEDOT modified GCE by electropolymerization and investigated the ORR catalytic mechanism. The results showed that the ORR could be catalyzed by PEDOT and proceeded via the 2-electrons pathway only in the alkaline media. As we all know, ORR has 2-electrons or 4-electrons transfer process in alkaline solution, and the latter is most effective pathway for ORR. So, it is significant that how to improve the number of transferred electrons of ORR on PEDOT.

GQDs, single- or few-layer graphene with a tiny size of several nanometers, have generated much excitement for a widely of promising applications in solar cells, fuel cells and others due to the remarkable quantum confinement and edge effects[21-23]. In recent years, GQDs, carbon nanodots (CNDs) and their corresponding composites (e.g., PtCu@GQDs, CuS/CNDs) synthesizes by various methods have been successfully used as ORR electro-catalysts[22, 24-29]. Nevertheless, the reported results indicate that an ORR electrode prepared by directly coating GQDs or CNDs electro-catalyst onto glassy carbon electrode (GCE) often suffers from poor stability and uniformity due to their high water dispersion property and easy aggregation[30].

In this work, based on the previous works[20, 31], we prepare the GQDs doped PEDOT ORR catalyst by electropolymerization and demonstrate that GQDs doping can improve the catalytic activity and stability of PEDOT.

2. EXPERIMENTAL

2.1 Chemicals

Sulfuric acid, nitric acid (analytical reagent, Beijing Chemical Plant), lithium perchlorate trihydrate, 3,4-ethylenedioxythiophene, graphene oxide, methanol, ethanol (purity ≥99%, Aladdin), sodium hydroxide (analytical reagent, Guangfu Technology Co. Ltd., Tianjin). For O_2 reduction measurement, highly purified O_2 (99.999%) was used. Deionized water was used throughout the experiments.

2.2 Preparation of GQDs

50 mg graphene oxide was heated at 300°C for 2 h to remove oxidation in N_2 atmosphere. The product was added into 10 mL concentrated sulfuric acid and 30 mL concentrated nitric acid. Then the system was treated by ultrasonication for 14 h. The mixture was added in 250 mL deionized water and filtered. The remaining solid was added in 40 mL deionized water and dispersed by ultrasonication for approximately 30 min to obtain a homogeneous suspension. The pH value of the solution was adjusted with sodium hydroxide to 8. The solution was transferred to a 50 mL PTFE reactor. The above system was heated at 200°C for 10 h. After that, it was cooled to room temperature and filtered with 0.22 μm microporous membrane. The GQDs was collected after the filtrate was dialyzed in a dialysis bag (cut-off molecular weight 3500 Da) for 12 h.

2.3 Structural characterization

The morphologies of PEDOT and GQDs@PEDOT were characterized by a HT7700 transmission electronic microscopy (Hitachi, Japan) at an acceleration voltage of 100 kV. Raman spectra were recorded using an InVia Raman Microscope (Renishaw, England) with an Ar laser at a wavelength of 532 nm.

2.4 Electrochemical measurements

The electrochemical measurements were performed in a three electrode system by using a CHI920D electrochemical workstation. A glass carbon electrode (GCE, 4 mm in diameter) loaded with the catalyst was used as the working electrode, an Ag/AgCl electrode as the reference electrode, and a Pt plate as the counter electrode. The electrolyte was 0.1 M NaOH solution. Prior to experiments, RDE was firstly polished by using 1.0, 0.3 and 0.05 μm alumina slurry sequentially, then rinsed adequately using deionized water and ethanol in ultrasonic bath, and dried in N_2 stream. The working electrode was prepared as follows. Firstly, 0.8 g lithium perchlorate trihydrate and 0.5 mL 3,4-ethylenedioxythiophene (EDOT) were added in 50 mL GQDs solution. Then, EDOT and aqueous solution were homogenized by sonication for 30 min. PEDOT was obtained by cyclic voltammetry in the mixed solution, which was used as electrolyte. A GCE was used as the working electrode, an Ag/AgCl electrode as the reference electrode, and a Pt plate as the counter electrode. Before tests, the electrode was rinsed using ethanol to remove residual EDOT monomer and dried under vacuum. The catalyst coated GCE was placed in an electrochemical cell containing 60 mL of N_2-saturated or O_2-saturated 0.1 M NaOH solution. By using the same electrode configuration, PEDOT catalyst were also studied for comparison.

The ORR measurements were performed in O_2-saturated 0.1 M NaOH electrolyte. Cyclic voltammograms curves (CVs) were recorded by applying a linear potential scan between -1.0 and 0 V at a sweep rate of 10 $mV \cdot s^{-1}$. The measurement curves were recorded when the cycling was repeated until the reproducible CV curves were obtained. Measurement on rotating disk electrode (RDE, 4 mm

in diameter) was carried out on a CHI920D electrochemical workstation at a scan rate of 10 $mV \cdot s^{-1}$. RDE measurements were conducted at different rotating speeds from 100 to 2000 rpm.

All electrochemical experiments were performed at room temperature. In CV, LSV and stability curves, current densities were normalized in reference to the geometric area of a RDE (0.1256 cm^2).

3. RESULTS AND DISCUSSION

3.1 Electropolymerization of EDOT in different media

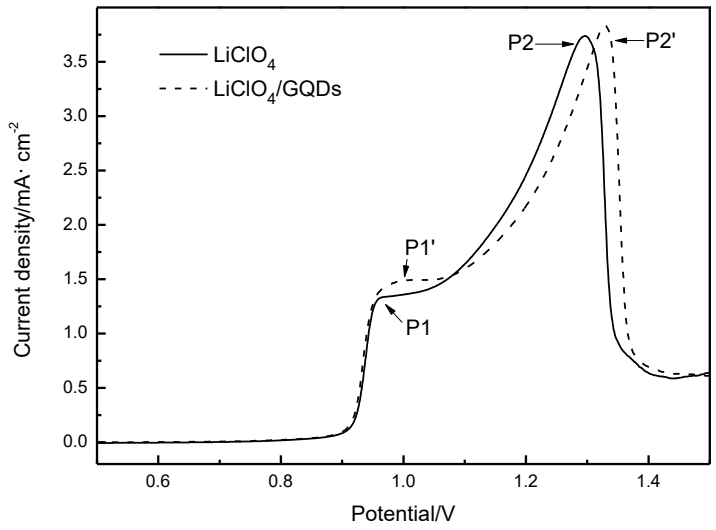

Figure 1. LSVs of EDOT on GCE in different media containing EDOT monomer at 10 $mV \cdot s^{-1}$

Figure 1 shows the LSVs of EDOT in different media at a sweep rate of 10 $mV \cdot s^{-1}$. In $LiClO_4$ media, two oxidation peaks (P1 and P2) were found at 0.97 and 1.29 V, respectively. The two peak potential values are in agreement with previously reported data[20]. The first peak is related to the oxidation of monomer, which adsorbed on or free from the electrode surface. The second peak is related to the oxidation of EDOT species diffused to the electrode closely, or the overoxidation of the PEDOT film as enough amount of polymer deposited on the electrode[31]. In order to provide a high driving force and avoid over oxidation, potential of 1.1 V was selected as the final potential.

In $LiClO_4$/GQDs media, two oxidation peaks (P1' and P2') were found at 1.01 and 1.33 V, respectively. Compared with P1 and P2, P1' and P2' shifted positively with a larger current density. This result indicated that GQDs had a hindrance to the electropolymerization process of PEDOT and the addition of GQDs increased the apparent area. So, a higher potential of 1.2 V was selected as the final potential.

3.2 Morphology and composition

Figure 2 shows the TEM images of PEDOT and GQDs@PEDOT. As can be seen from Figure 2a, PEDOT had a catenulate structure, which was very consistent with the previous report[32]. In the Figure 2b, GQDs gathered on the edge of PEDOT and incorporated into PEDOT tightly with a fairly average particle size of 3-5 nm. The high water dispersion property of GQDs has been improved obviously. PEDOT film in the aggregation area of GQDs was relatively thin due to the hindrance of GQDs. This result was in accordance with 3.1. Therefore, the addition of GQDs increased the specific surface area of the catalyst and was expected to benefit the improvement of electrocatalytic activity.

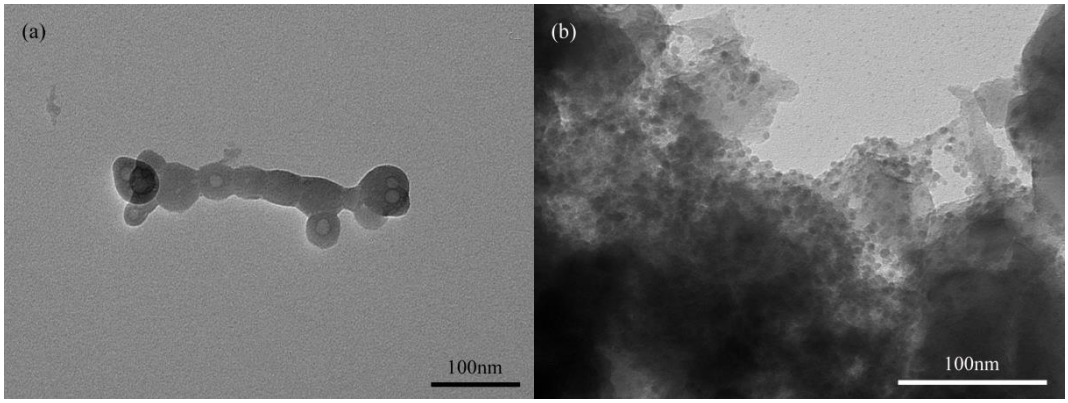

Figure 2. TEM images of (a) PEDOT and (b) GQDs@PEDOT

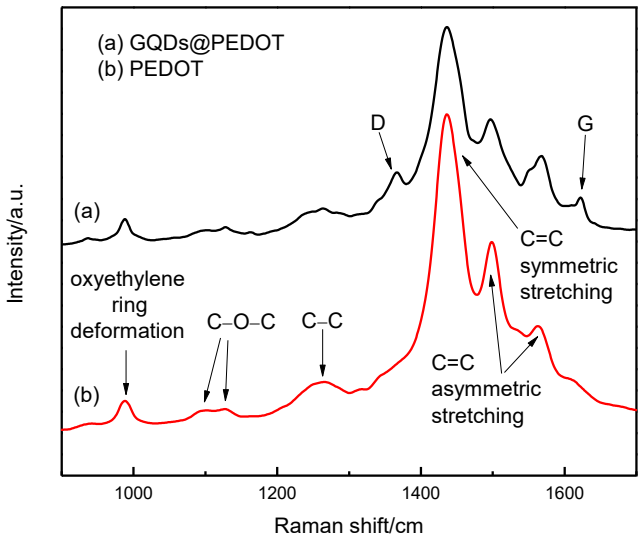

Figure 3. Raman spectra of PEDOT and GQDs@PEDOT. Laser excitation wavelength: 532 nm

Raman is often used to verify that GQDs has been incorporated into electroactive conducting polymers (ECPs) films[33]. Figure 3 shows the Raman spectra of PEDOT and GQDs@PEDOT films. The Raman spectra of the PEDOT film had three strong bands at 1563, 1499 and 1435 cm^{-1} attributed

to the asymmetric and symmetric C=C stretch. The band at 1264 cm^{-1} originated from the C_{α}–$C_{\alpha'}$ inter-ring stretch, the bands at 1097 and 1127 cm^{-1} from the C–O–C deformation, and finally the band at 988 cm^{-1} from the oxyethylene ring deformation[33-35]. Besides, the GQDs@PEDOT spectra consisted of two bands centered at 1621 and 1365 cm^{-1} that were attributed to the well-documented G and D bands of GQDs[36]. The presence of D band is negligible in graphite. However, its appearance in the GQDs can be ascribed to the structural imperfections of –COOH groups and the partially disordered crystal structure due to the small sp^2 cluster size[36]. Thus, the value of I_D/I_G ratio can be used as a marker to identify the formation of GQDs. The I_D/I_G ratio for the synthesized GQDs was significantly higher (0.91) than that of graphite (~0.1)[36] signifying the efficiency of the proposed synthesis method. This suggested, not only that GQDs had been successfully incorporated in the PEDOT film, but also that the GQDs dispersion was a suitable electropolymerization medium for PEDOT[33].

3.3 Electrocatalytic performance

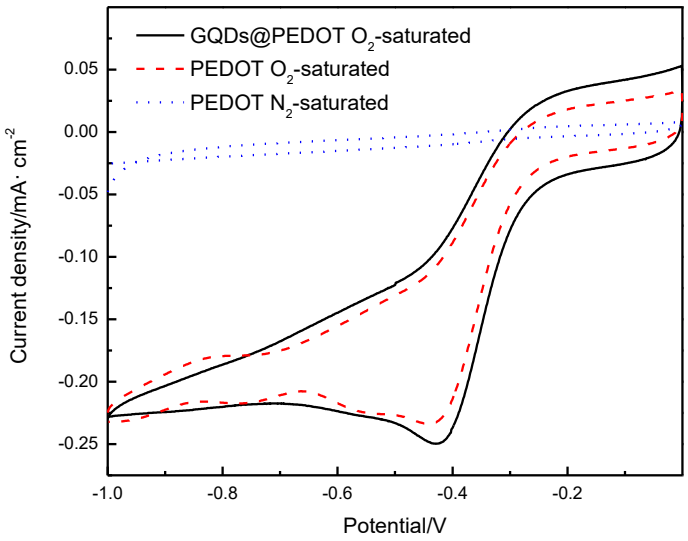

Figure 4. CV curves of PEDOT and GQDs@PEDOT in O_2 or N_2 saturated 0.1 M NaOH solution at a scan rate of 10 $mV \cdot s^{-1}$

Figure 4 confirms the oxygen reduction activity of the catalysts in the O_2 or N_2 saturated 0.1 M NaOH solution. For the PEDOT, the onset potential of ORR is at -0.24 V with a single cathodic reduction peak at around -0.44 V. For the GQDs@PEDOT catalyst, its reduction peak potential (-0.42 V) and the onset potential (-0.2 V) of ORR showed a positive shift slightly with a more pronounced increase in the current density. When the electrolyte was saturated with N_2, there was not any cathodic reduction peak on the CV curve. These results indicated the PEDOT was an effective ORR catalyst, meanwhile GQDs@PEDOT showed an enhancement in the ORR electrocatalytic activity.

To further investigate the ORR performance, polarization curves for the ORR on two catalysts are shown in Figure 5. As can be seen, the ORR onset potentials at the two catalysts were around -0.2 V, followed by a continuous increase in the current density. The strongest limiting diffusion current density on GQDs@PEDOT electrode (-1.62 mA·cm^{-2}) was bigger than PEDOT electrode (-1.33 mA·cm^{-2}). This result was probably due to the efficient four-electron pathway[37].

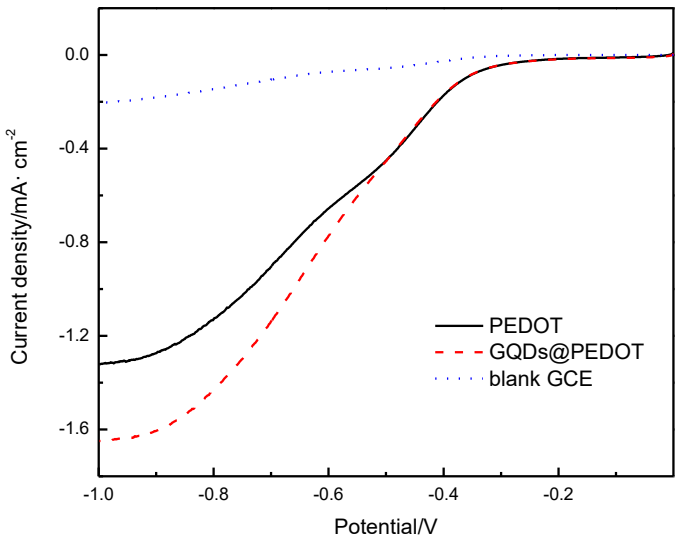

Figure 5. LSV curves of PEDOT, GQDs@PEDOT and blank GCE with a RDE at rotating speed of 1600 rpm and scan rate of 10 mV·s^{-1}

It is well known that the transferred electron number in an ORR process is an important parameter to determine the efficiency of an electro-catalyst. For the ORR at a RDE, the Koutecky-Levich equation can be described as follows[38]:

$$i^{-1}=i_k^{-1}+i_j^{-1}=i_k^{-1}+(Bw^{1/2})^{-1} \quad (1)$$

where i is the disk currents, i_j is the diffusion-limiting current, i_k is kinetic current, w is the electrode rotation rate (rad/s) and B is Levich slope that is given by:

$$B=0.62nFAD_{O_2}^{2/3}v^{-1/6}C_{O_2} \quad (2)$$

where n is the number of transferred electrons of per oxygen molecule, F is the Faraday constant (96485 C·mol^{-1}), A the geometric surface area of the electrode, v is the kinetic viscosity for NaOH (0.011 cm^2·s^{-1}), C_{O_2} is the concentration of O_2 (1.2×10^{-3} mol·L^{-1}) and D_{O_2} is the diffusion coefficient of O_2 in 0.1 M NaOH (1.9×10^{-5} cm^2·s^{-1})[39].

Figure 6 and Figure 7 show the LSV responses of the PEDOT and GQDs@PEDOT coated GCE in an O_2-saturated 0.1 M NaOH solution under different rotation rates with a sweep rate of 10 mV·s^{-1}. As shown, the cathodic current density increased with increasing rotation rate (from 100 rpm to 2000 rpm) due to the enhanced diffusion of electrolytes. What is more, the limiting current densities obtained from the GQDs@PEDOT were higher than PEDOT at a constant rotation rate. The n was also calculated from the slope of the K-L plots to be 3.57 for GQDs@PEDOT, which closed to the

theoretical value 4. The comparison of the electrocatalytic performances with similar ORR electrocatalysts was summarized in Table 1. According to Table 1, the electron-transfer number for ORR on GQDs@PEDOT electrode was higher than that on the other electrocatalyst. The results showed that the interaction of GQDs with PEDOT largely contributed the electrocatalytic activity of GQDs@PEDOT. This is probably due to the abundant defective sites on surface of GQDs, which not only serve as an anchoring point for PEDOT components, but also enhance the interaction of PEDOT with O_2 by relatively weakening O_2 adsorption energy[40].

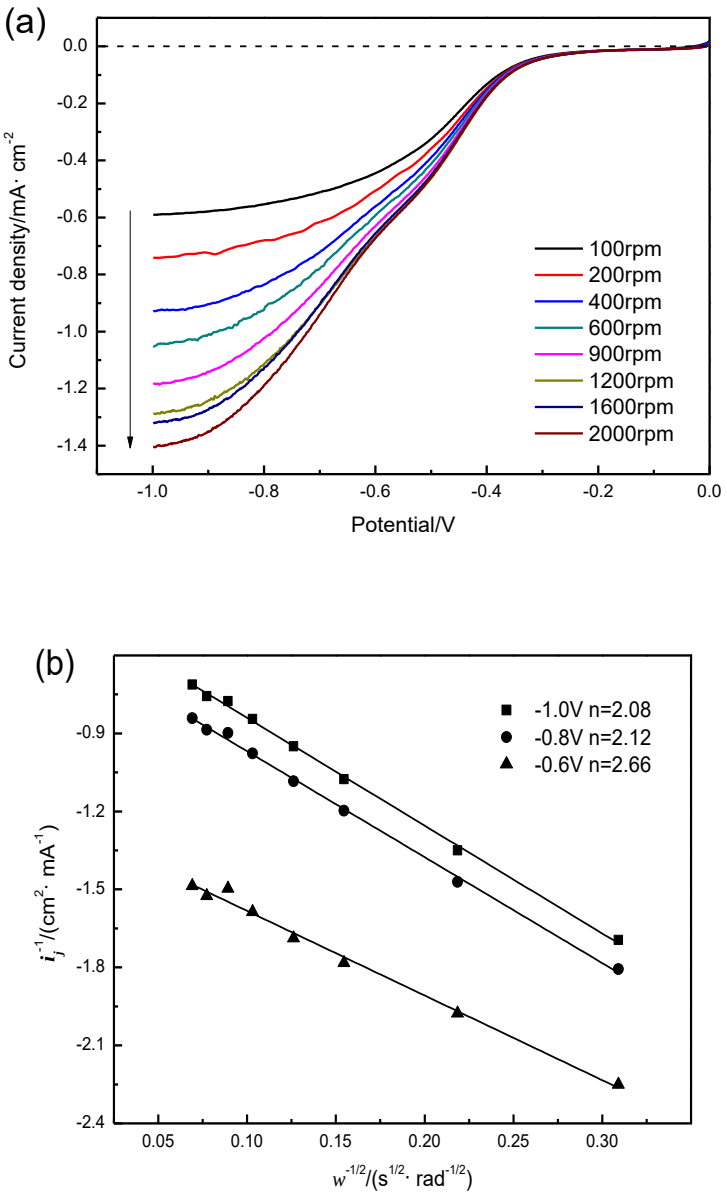

Figure 6. (a) LSVs obtained for PEDOT at various rotating speeds; (b) Koutecky–Levich plots for PEDOT obtained from LSVs in (a) at different potentials

Table 1. The comparison of the electrocatalytic performances with similar ORR electrocatalysts

ORR electrocatalyst	electrolyte	electron-transfer number (n)	Ref.
PEDOT	0.1 M KOH	2	[31]
PEDOT:PSS	0.1 M KOH	2.1	[19]
PEDOT/rGO	0.1 M KOH	2.5	[19]
PEDOT:PSS/rGO	0.1 M KOH	3.3	[19]
GQDs@PEDOT	0.1 M NaOH	3.57	This work

In addition, the durability of the PEDOT and GQDs@PEDOT electrodes for ORR was evaluated by a chronoamperometric method at -0.5 V in O_2 saturated 0.1 M NaOH at a rotation rate of 1600 rpm. As shown in the Figure 8, the current density loss on GQDs@PEDOT was much less than that on PEDOT after continuous reaction for 5000 s. The current densities of GQDs@PEDOT and PEDOT at 5000 s were 0.26 and 0.19 $mA \cdot cm^{-2}$.

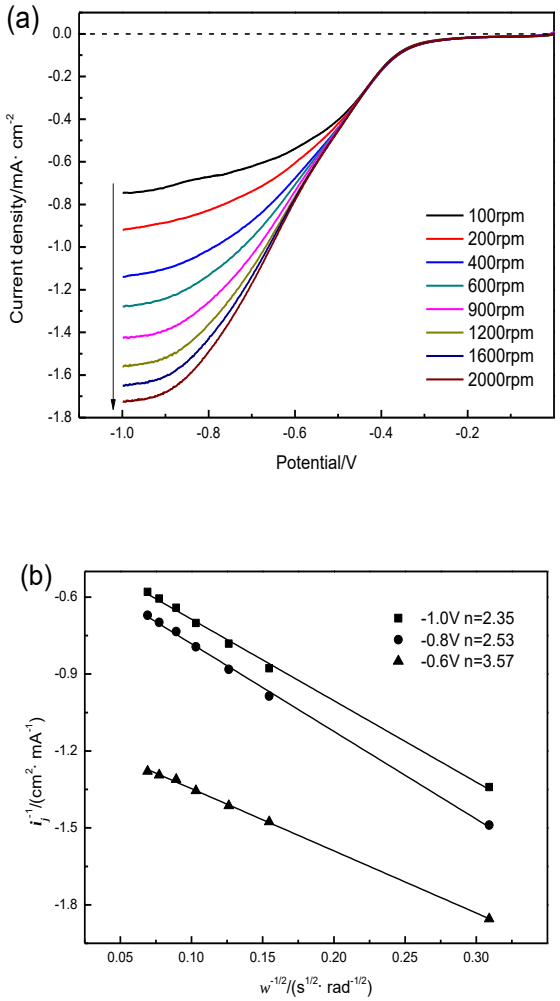

Figure 7. (a) LSVs obtained for GQDs@PEDOT at various rotating speeds; (b) Koutecky–Levich plots for GQDs@PEDOT obtained from LSVs in (a) at different potentials

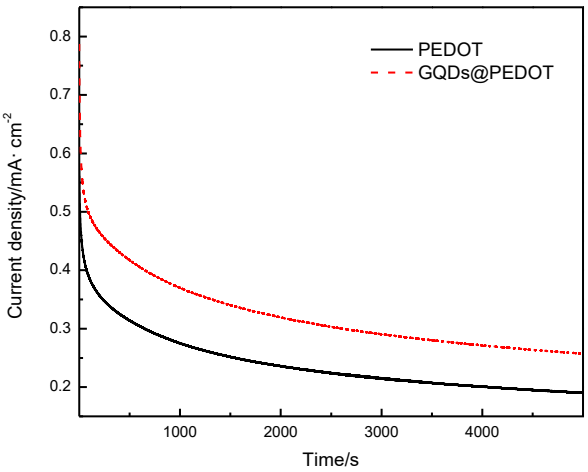

Figure 8. Current-time chronoamperometric response of PEDOT and GQDs@PEDOT in O_2 saturated 0.1 M NaOH solution with a rotating speed of 1600 rpm

The stability of GQDs@PEDOT was clearly greater than PEDOT. These results further demonstrate that the GQDs doping with PEDOT can enhance not only the catalytic activity, but also the stability toward ORR.

4. CONCLUSION

In summary, PEDOT and GQDs@PEDOT ORR catalysts were prepared by the electropolymerization. TEM images showed the GQDs had been incorporated in the PEDOT film successfully and its high water dispersion property has been inhibited clearly. At the same time, the addition of GQDs increased the specific surface area of catalyst. After GQDs doped, the number of transferred electrons increased from 2.66 to 3.57 and the current density at 5000 s increased from 0.19 to 0.26 $mA \cdot cm^{-2}$. The GQDs@PEDOT performed remarkably enhanced catalytic activity and stability in ORR better than PEDOT probably due to the interaction of GQDs with PEDOT.

ACKNOWLEDGEMENTS
This work was supported by Natural Science Foundation of Ningxia, China (No. NZ14097), Science and Technology Research Project of Ningxia Colleges (NGY2016163), Chinese Academy of Sciences (CAS) "Light of West China" Program and Natural Science Foundation of China (No. 61461001).

References

1. Y. He, C. Zhu, K. Chen, J. Wang, H. Qin, J. Liu, S. Yan, K. Yang and A. Li, *J. Power Sources*, 339 (2017) 13.
2. M. V. Kannan and G. Gnana Kumar, *Biosens. Bioelectron.*, 77 (2016) 1208.
3. Y. Zhou and Y. Wang, *J. CIESC*, 68 (2017) 519.
4. M. K. Carpenter, T. E. Moylan, R. S. Kukreja, M. H. Atwan and M. M. Tessema, *J. Am. Chem. Soc.*, 134 (2012) 8535
5. H. Yang, *Angew. Chem. Int. Ed.*, 50 (2011) 2674.
6. Y. Xue, H. Miao, S. Sun, Q. Wang, S. Li and Z. Liu, *J. Power Sources*, 342 (2017) 192.

7. Y. Xue, S. Sun, Q. Wang, H. Miao, S. Li and Z. Liu, *Electrochim. Acta*, 230 (2017) 418.
8. D. M. F. Santos, T. F. B. Gomes, B. Šljukić, N. Sousa, C. A. C. Sequeira and F. M. L. Figueiredo, *Electrochim. Acta*, 178 (2015) 163.
9. B. Liu, B. Huang, C. Lin, J. Ye and L. Ouyang, *Appl. Surf. Sci.*, 411 (2017) 487
10. Z. Wang, M. Li, L. Fan, J. Han and Y. Xiong, *Appl. Surf. Sci.*, 401 (2017) 89
11. X. Yuan, X. Ding, C. Wang and Z. Ma, *Energ. Environ. Sci.*, 6 (2013) 1105.
12. Z. Yang, H. Nie, X. Chen, X. Chen and S. Huang, *J. Power Sources*, 236 (2013) 238.
13. J. P. Paraknowitsch and A. Thomas, *Energ. Environ. Sci.*, 6 (2013) 2839.
14. C. Huang, C. Li and G. Shi, *Energ. Environ. Sci.*, 5 (2012) 8848.
15. D. Su, S. Perathoner and G. Centi, *Chem. Rev.*, 113 (2013) 5782.
16. C. Zhai, M. Sun, M. Zhu, S. Song and S. Jiang, *Appl. Surf. Sci.*, 407 (2017) 503.
17. K. Gong, F. Du, Z. Xia, M. Durstock and L. Dai, *Science*, 323 (2009) 760.
18. B. Winther-Jensen, O. Winther-Jensen, M. Forsyth and D. R. Macfarlane, *Science*, 321 (2008) 671.
19. M. Zhang, W. Yuan, B. Yao, C. Li and G. Shi, *ACS Appl. Mater. Interfaces*, 6 (2014) 3587.
20. J. Ma, X. Wang and X. Jiao, *Int. J. Electrochem. Sci.*, 7 (2012) 1556.
21. K. Kakaei, H. Javan, M. Khamforoush and S. A. Zarei, *Int. J. Hydrogen Energy*, 41 (2016) 14684.
22. L. Wang, C. Hu, Y. Zhao, Y. Hu, F. Zhao, N. Chen and L. Qu, *Carbon*, 74 (2014) 170.
23. J. K. Kim, M. J. Park, S. J. Kim, D. H. Wang, S. P. Cho, S. Bae, J. H. Park and B. H. Hong, *ACS nano*, 7 (2013) 7207.
24. Q. Li, S. Zhang, L. Dai and L. Li, *J. Am. Chem. Soc.*, 134 (2012) 18932.
25. Z. Y. Shih, A. P. Periasamy, P. C. Hsu and H. T. Chang, *Appl. Catal. B: Environ.*, 132-133 (2013) 363.
26. M. Liu and W. Chen, *Nanoscale*, 5 (2013) 12558.
27. J. Cao, Y. Hu, L. Chen, J. Xu and Z. Chen, *Int. J. Hydrogen Energy*, 42 (2017) 2931.
28. H. Zhang, Y. Wang, D. Wang, Y. Li, X. Liu, P. Liu, H. Yang, T. An, Z. Tang and H. Zhao, *Small*, 10 (2014) 3371.
29. H. Liu, Q. Zhao, J. Liu, X. Ma, Y. Rao, X. Shao, Z. Li, W. Wu, H. Ning and M. Wu, *Appl. Surf. Sci.*, 423 (2017) 909.
30. H. Zhang, J. Chen, Y. Li, P. Liu, Y. Wang, T. An and H. Zhao, *Electrochim. Acta*, 165 (2015) 7.
31. J. Ma, T. Xue, Z. Zou, B. Wang and M. Luo, *Int. J. Electrochem. Sci.*, 10 (2015) 4562.
32. W. Zhou, X. Hu, X. Bai, S. Zhou, C. Sun, J. Yan and P. Chen, *ACS Appl. Mater. Interfaces*, 3 (2011) 3839.
33. A. Österholm, T. Lindfors, J. Kauppila, P. Damlin and C. Kvarnström, *Electrochim. Acta*, 83 (2012) 463.
34. T. Lindfors, Z. A. Boeva and R.-M. Latonen, *RSC Advances*, 4 (2014) 25279.
35. A. García-Barberá, M. Culebras, S. Roig-Sánchez, C. M. Gómez and A. Cantarero, *Synth. Met.*, 220 (2016) 208.
36. S. K. Tuteja, R. Chen, M. Kukkar, C. K. Song, R. Mutreja, S. Singh, A. K. Paul, H. Lee, K. H. Kim, A. Deep and C. R. Suri, *Biosens. Bioelectron.*, 86 (2016) 548.
37. S. Wang, D. Yu and L. Dai, *J. Am. Chem. Soc.*, 133 (2011) 5182.
38. Y. Li, Y. Zhao, H. Cheng, Y. Hu, G. Shi, L. Dai and L. Qu, *J. Am. Chem. Soc.*, 134 (2012) 15.
39. S. M. Kim, Y. G. Jo, M. H. Lee, N. Saito, J. W. Kim and S. Y. Lee, *Electrochim. Acta*, 233 (2017) 123.
40. D. H. Lim and W. Jennifer, *J. Phys. Chem. C*, 116 (2012) 3653.